52nd IEEE Conference on Decision and Control
December 10-13, 2013. Florence, Italy

Sliding Mode and Fuzzy Logic Control for Heaving Wave Energy Converter

Addy Wahyudie[1], Muhammad Abdi Jama[1], Ali Assi[2], and Hassan Noura[1]

Abstract— **This paper proposes two control strategies for controlling the heaving wave energy converter (WEC): sliding mode control (SMC) and fuzzy logic control (FLC). The two methods are implemented to maximize the absorbed energy of the heaving WEC. This can be achieved by designing the control laws so that the buoy's velocity follows its reference. The two control strategies are tested using actual polychromatic ocean wave. The control strategies consider the physical limitation of the control force and the buoy's elevation. Finally, the performances of the two control methods are tested and compared in the nominal and perturbation scenarios.**

I. INTRODUCTION

Recently, the generation of electricity from ocean waves has gained an increasing attention. It is estimated that oceans have potential power up to 10 [TW] [1]. The average power intensity is $2-3$ [kw/m^2 which is almost $4-6$ times bigger than the wind energy (0.5 [kW/m^2]) [2]. Wave Energy Converter (WEC) is the device that transforms the mechanical energy carried by the wave into electrical power. The simplest structure of the WEC is a point body or heaving WEC, as depicted in Fig. 1. The heaving WEC consists of a floater or buoy that connected to permanent magnet linear generator (PMLG) using a rod [3]. The PMLG is used as power take-off (PTO) mechanism and as controller that provides optimum power generation and robustness properties for the structure against uncertainties/external disturbances [4].

Many papers have been published relating to WEC's control. For example, papers [5-6] showed that an efficient heaving WEC must oscillate oscillate with same frequency of the incident waves. Papers [7-8] concluded that resonance occurs when the body velocity is in phase with the wave excitation. In [9], the authors proposed a fuzzy logic control (FLC) to control the damping and stiffness of the PTO mechanism. TIn this work, auto-tuning FLC is used with genetic algorithm based on stored data. Auto-tuning FLC using particle swarm optimization to control WEC can be found in [10-11]. Latching control is proposed by Budal and Falnes in [5]. The mechanism of latching control consists of locking the oscillating body when the velocity becomes zero, and unlocking it when maximum or minimum velocity is anticipated. Few research efforts have been dedicated recently to use model predictive control in controlling WECs [12-14].

In this paper, we propose a sliding mode control (SMC) and a FLC for controlling the heaving WEC. The SMC strategy is used because of its capability to track the reference input and robustness property against parameter perturbation of the model and external disturbance. The FLC is well known of its capability to add the expert knowledge about a system using linguistic inputs/outputs rather than using mathematical expressions. Moreover, the form of the reference input is a sinusoidal wave with multiple amplitudes and frequencies. Therefore, conventional control methods, for example: PID and state feedback control, can not be used for this purpose. In order to provide viable control solution for heaving WEC, we use the fixed (non auto-tuning) FLC. Therefore, the proposed methods are both fixed controllers and have low computation cost when implemented.

The paper is organized as follows. Section II discusses the dynamic model of heaving WEC. The proposed control strategies are described in Section III. The simulation results and comparison of the two control strategies are presented in Section IV. Finally, conclusions are given in Section V.

II. DYNAMIC MODEL OF HEAVING WEC

Basically, there are two steps to obtain the dynamic model of heaving WEC, i.e., the derivation of the WEC model in time domain and the system identification of its parameters using the hydrodynamic analysis. In practical, the model of heaving WEC is highly non-linear system. This is due to the non-linear properties of the incident waves and forces acting in the PTO [6]. However, we can linearize this non-linear dynamic of the WEC around its operating point where only small excursion of the buoy is allowed.

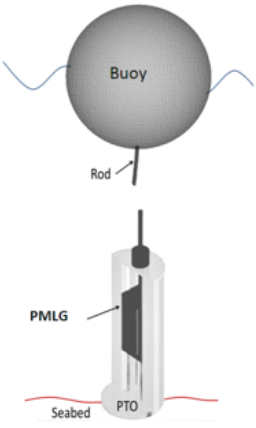

Fig. 1. Heaving point absorber structure.

[1]Addy W, M. A. Jama, H. Noura are with the Electrical Engineering Department, United Arab Emirates University, P.O. Box 15551 Al Ain, UAE addy.w at uaeu.ac.ae

[2]A. Assi is with the Department of Electrical and Electronic Engineering, Lebanese International University, Beirut, Lebanon

The motion equation of the buoy is formulated as

$$f_e(t) - f_r(t) - f_b(t) - f_{los}(t) - f_u(t) = [m + m_\infty]\ddot{z}(t) \quad (1)$$

where m is the total mass of the WEC's buoy and the PMLG translator, m_∞ is the infinite added mass, $\ddot{z}(t)$ is the gravitational vertical acceleration of the buoy, $f_e(t)$ is the wave excitation force, $f_r(t)$ is the wave radiation force, $f_b(t)$ is the buoy's buoyancy force, $f_{los}(t)$ is the mechanical losses force, and $f_u(t)$ is the control machinery force applied by the PMLG [15]. The buoyancy force, f_b can be formulated as

$$f_b(t) = c_b z(t)$$

where the constant c_b and z are the buoyancy stiffness coefficient and the buoy's vertical displacement, respectively. The radiation force, f_r is calculated based on the following formula

$$f_r(t) = \int_0^t (t-\tau)\dot{z}(\tau)d\tau,$$

where $\dot{z}$ is the vertical velocity of the buoy. Neglecting the mechanical losses $f_{los}(t)$, the time domain equation for the motion of a zero forward speed freely heaving buoy in (1) can be re-written as

$$[m + m_\infty]\ddot{z}(t) + \int_0^t (t-\tau)\dot{z}(\tau)d\tau + c_b z(t) + f_u(t) = f_e(t).$$

From the latter equation, there are two types of the WEC's inputs, the control force f_u and the wave excitation force f_e. The control force can be modified by the controller, while the excitation force cannot be modified by control action. In [16], authors suggested the radiation convolution term can be approximated by a n-th order state space model. Here, we use 4th order state space model to approximate the convolution term in the radiation force.

Therefore, the system state space representation becomes:

$$\begin{aligned} \dot{\mathbf{x}}(\mathbf{t}) &= \mathbf{A}\mathbf{x}(\mathbf{t}) + \mathbf{B}\mathbf{u}(\mathbf{t}) \\ \mathbf{y}(\mathbf{t}) &= \mathbf{C}\mathbf{x}(\mathbf{t}) \end{aligned} \quad (2)$$

where $x(t) = [z(t) \quad \dot{z}(t) \quad \boldsymbol{\theta}(t)]^T \in \mathbb{R}^{(6\times 1)}$ is the system state vector, $\boldsymbol{\theta}(t) \in \mathbb{R}^{(1\times 4)}$ is the radiation component state vector. State variables $y(t) = [z(t) \quad \dot{z}(t)]^T \in \mathbb{R}^{(2\times 1)}$ is the output vector. **A**, **B**, and **C** are the state, input and output matrices, respectively. The matrices in (2) are written as

$$\mathbf{A} = \begin{bmatrix} 0 & 1 & \mathbf{0_{1\times 4}} \\ \frac{-c_b}{m+m_\infty} & 0 & \frac{-\mathbf{C_k}}{m+m_\infty} \\ \mathbf{0_{4\times 1}} & \mathbf{B_k} & \mathbf{A_k} \end{bmatrix} \in \mathbb{R}^{6\times 6},$$

$$\mathbf{B_u} = \begin{bmatrix} 0 & 0 \\ \frac{1}{m+m_\infty} & -\frac{1}{m+m_\infty} \\ \mathbf{0_{4\times 1}} & \mathbf{0_{4\times 1}} \end{bmatrix} \in \mathbb{R}^{6\times 2},$$

$$\mathbf{C} = \begin{bmatrix} 1 & 0 & \mathbf{0_{1\times 4}} \\ 0 & 1 & \mathbf{0_{1\times 4}} \end{bmatrix} \in \mathbb{R}^{2\times 6}.$$

The next step is how to determine the matrices $\mathbf{A_k}$, $\mathbf{B_k}$ and $\mathbf{C_k}$ in the latter equation. The matrices $\mathbf{A_k} \in \mathbb{R}^{(4\times 4)}$, $\mathbf{B_k} \in \mathbb{R}^{(4\times 1)}$, and $\mathbf{C_k} \in \mathbb{R}^{(1\times 4)}$ are the radiation component state and input matrices, which are determined by linearly approximating the frequency domain radiation kernel $K_r(\omega)$ using frequency response identification [17-18]. $K_r(\omega)$ can be written as

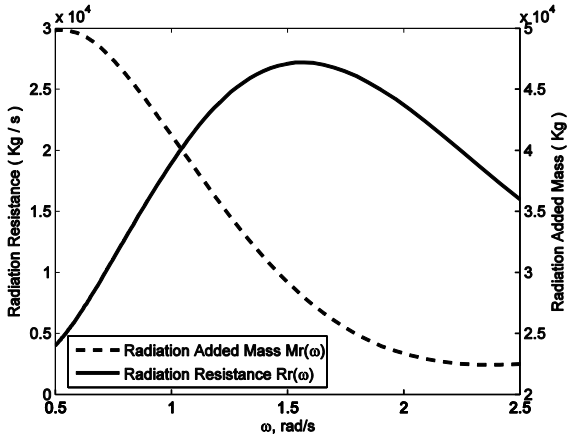

Fig. 2. Spherical buoy hydrodynamic parameters.

$$K_r(\omega) = R_r(\omega) + j(\omega)[M_r(\omega) - m_\infty]$$

where $R_r(\omega)$ and $M_r(\omega)$ are the radiation resistance and the radiation added mass, respectively. Special software, for example WAMIT^{TM} which is a boundary element method based software [18], can be used to compute $R_r(\omega)$ and $M_r(\omega)$ for a range of wave frequencies as shown in Fig. 2. From this Section, we drop the variable t in all formulation for the sake of simplicity.

III. CONTROLLER DESIGN

The control system configuration is shown in Fig. 3. The excitation force generator converts the wave ocean elevation η into excitation force f_e using the method described in [16]. The buoy's velocity reference $\dot{z}_r$ is obtained by converting f_e using the reference signal generator. The reference signal generator is obtained by following equation

$$\dot{z}_r = \frac{1}{2R_r} f_e.$$

The proposed control strategy C receives the input in term of the error $\dot{e}$ and its derivative $\ddot{e}$, where $\dot{e}$ is the error between $\dot{z}_r$ with the buoy's velocity $\dot{z}$.

The outline of this Section is follows. First, we will described the proposed SMC. After that, the FLC is given for the sake of comparison.

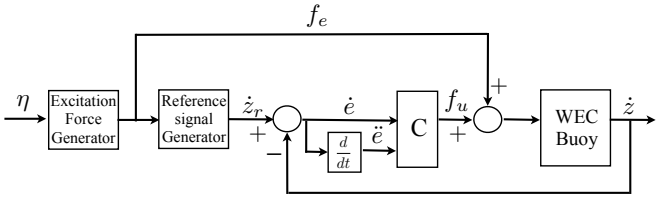

Fig. 3. Proposed control system configuration.

A. Sliding Mode Control for WEC

The proposed SMC consists of two major parts, i.e, low frequency part f_l and high frequency part f_h or

$$f_u = f_h + f_l. \tag{3}$$

The low frequency part of the controller only is enough to make the velocity of the buoy follows its reference, in the case nominal system (perfect modeling). The high frequency part is needed as robustness compensator in the controlled system.

The derivation of the low frequency part of the SMC is given in [19]. Let define the error e as

$$e = z - z_r.$$

The motion of the buoy is governed by the following forces

$$\ddot{z} = \frac{1}{(m + m_\infty)}[f_e - f_r - f_b - f_l] \tag{4}$$

where we replace f_u with f_l for the nominal case. Let us define the sliding surface s as

$$s = \left(\frac{d}{dt} + \lambda\right)^{n-1} e = 0.$$

Here λ is strictly positive constant representing the speed of convergence e in a sliding surface. For the second order system, sliding surface can be formulated as

$$s = \dot{e} + \lambda e = 0.$$

Differentiating the last equation, the following equation can be obtained

$$\dot{s} = \ddot{e} + \lambda\dot{e} = (\ddot{z} - \ddot{z}_r) + \lambda\dot{e} = 0.$$

Substituting the latter equation with (4), the low frequency component of the controller is given by the following equation

$$f_l = \frac{1}{(m + m_\infty)}[f_e - f_r - f_b - \ddot{z}_{ref} + \lambda\dot{e}]. \tag{5}$$

In order to preserve robustness of the controlled system, f_h has been added in the control policy in the form of

$$f_h = k\ \mathrm{sgn(s)}$$

where sgn is the signum function:

$$\begin{aligned} \mathrm{sgn(s)} &= +1 \quad \text{if } s > 0 \\ \mathrm{sgn(s)} &= -1 \quad \text{if } s < 0. \end{aligned}$$

The constant k is a positive real constant and its value is large enough to compensate perturbations in the model. The larger values of k compensate the larger set of perturbations. However, this makes the control force also large. Therefore, the optimum value of k is chosen so that it is enough to compensate reasonable value of perturbations but still keeps the level of f_u below its maximum value. Therefore, the SMC equation can be written as

$$f_u(t) = f_l(t) + k\ \mathrm{sat(s/\Phi)}. \tag{6}$$

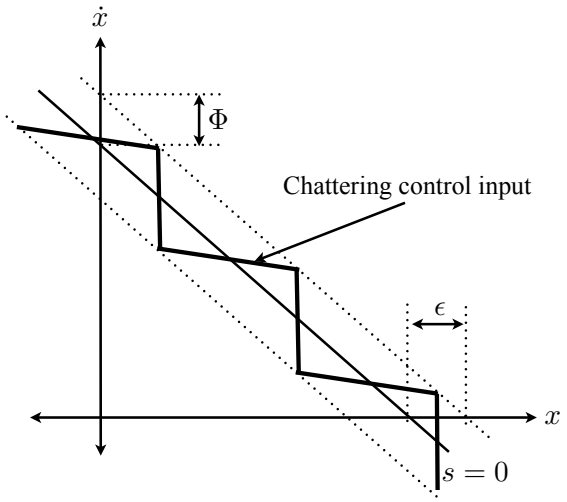

Fig. 4. Sliding surface with chattering control input.

The addition of the signum function in the last equation produces chattering control force. From practical point of view, this condition is undesirable because the actuator cannot follow the sudden change of the control force. The chattering control force can be smoothed using the method explained in [21]. Let us define a thin boundary layer neighboring the switching surface

$$B(t) = \{\mathbf{x}, |s(\mathbf{x}; t)| \leq \Phi\} \qquad \Phi > 0$$

where $\mathbf{x}$ is a state in sliding plane, in our case$\dot{z}$ and $\ddot{z}$. Φ is the boundary layer thickness and $\epsilon = \Phi/\lambda^{n-1}$ is the boundary layer width, as depicted in Fig. 4. $B(t)$ is a layer that contains the chattered control input. The chattered control input in $B(t)$ is interpolated by replacing the term $\mathrm{sgn(s)}$ by $\mathrm{sat\ s/\Phi}$. Therefore, the final form of the robust SMC with continuous control input for the system is formulated as

$$f_u(t) = f_l(t) + k\ \mathrm{sat(s/\Phi)}. \tag{7}$$

In order to implement f_u in term of stiffness and damping forces, we can put weighting value between b_u and c_u. In practical, the value of b_u is selected larger than c_u [9]. The damping force helps in making the buoy adjust its amplitude, while the stiffness force makes the buoy adjust its phase.

B. Fuzzy Logic Control for WEC

For the sake of comparison with the SMC, the FLC for the WEC is also proposed [[10-12]. Here, we use the fixed (non autotuning) FLC for the WEC. This because we will make the comparison between the two fixed controllers for the WEC. From the practical point of view, fixed order controller is used because of its low computation cost. The control force f_u is decomposed into two forces: damping and stiffness force [9]. The control force is given by

$$f_u = -b_u\dot{z} + c_u z \tag{8}$$

where b_u and c_u denote the damping and the spring stiffness coefficients. The control strategy continuously alters the

coefficients b_u and c_u so that the buoy's velocity follows its velocity.

The FLC consists of four essential elements which are:

1) Fuzzification: This process is to convert the crisp inputs into fuzzified linguistic variables.
2) IF-THEN rule: set of rules based on the expert knowledge about the controlled systems. The rule thats connects between the fuzzy inputs and fuzzy outputs.
3) Inference system: in which operations are carried on the provided rules to infer a decision.
4) Defuzzification: the process of converting the fuzzy variable into its crisp/numerical value.

In the proposed FLC for the WEC, the controller receives two inputs in the form of e and $\dot{e}$. The outputs of the FLC are the coefficients of b_u and c_u. In order to have sufficient resolution for the changes of the inputs and its effect on the outputs, we divide the fuzzy sets of the inputs and outputs into seven linguistic variables. We define the linguistic variables as NB (Negative Big), NM (Negative Medium), NS (Negative Small), Z (Zero), PS (Positive Small), PM (Positive Medium), PB (Positive Big). The range of universe of discourse of the inputs and outputs are selected to cover all possibility of the values for the input and outputs sets. Here, we use the Mamdani method in the inference system. The centroid method is used the defuzzification.

IV. SIMULATION RESULT AND DISCUSSION

In this section, the computer simulation setups and the simulation parameters of the control strategies are described. First, the two proposed methods are tested under nominal model condition. Then, we simulate the control methods with perturbation parameter introduced in the WEC model.

A. Simulation Setup

The setup for the WEC are designed to simulate using the real ocean environment. We use polychromatic ocean wave state (i.e, ocean's wave with multiple amplitudes and frequencies) as the input (η) for the simulations. The polychromatic sea state is formed using the JONSWAP spectrum with maximum heigh and maximum frequency are 1.5 [m] and 0.5 [rad/s], respectively [2]. The geometrical parameters for the buoy are given in Table I. The draft indicates the portion of the buoy under the water. The simulations are built using Matlab/Simulink environment [20]. The duration of simulations are 140 [sec] and the control actions are applied at 0 [sec]. The fixed step ode4 is used to compute the dynamic response of the simulation.

The fuzzy sets of inputs and outputs are depicted in Figure 5 and 6, respectively. The universe of discourse of e and $\dot{e}$ are [-3, 3] and [-5, 5], respectively. The universe of discourse of the fuzzy outputs b_u and c_u are $[-1 \times 10^5,\ 1 \times 10^5]$ and $[-1.5 \times 10^5,\ 1.5 \times 10^5]$, respectively. The seven linguistic variables from NB to PB in the form Gaussian membership function are distributed equally within the universe of discourses. The universe of discourse of e is selected between [-3, 3] to represent desirable displacement of the buoy relative to the height of η. The maximum

TABLE I
GEOMETRICAL PARAMETERS OF THE BUOY, THE SEA STATE CHARACTERISTICS, AND THE SMC

Shape	Sphere
Radius	4 [m]
Draft	4 [m]
Seabed depth	60 [m]
Wave period range	$1 - 13$ [sec]
λ	1
k	1×10^6
Φ	1×10^4

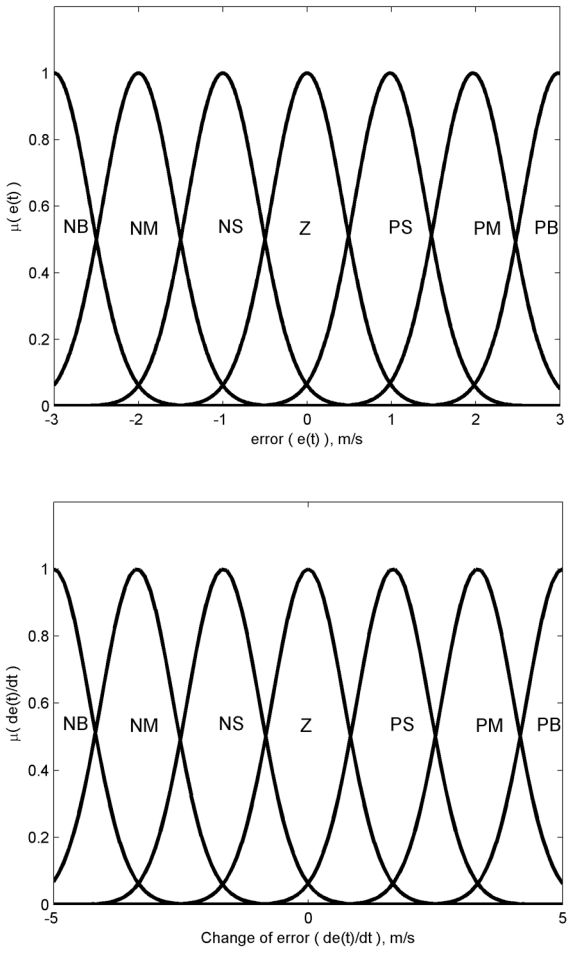

Fig. 5. Fuzzy sets for the input of the proposed FLC.

allowable displacement of the buoy is [-4, 4], this indicates that the buoy is not entirely jump/submerged from the wave surface. The displacement outside this range is not desirable due to the limitation of the physical rod between the PLMG and the buoy. The IF-THEN rules that connects the fuzzy inputs and outputs are described in Table II.

B. Simulation Result

Let us discuss the nature of buoy's elevation and velocity compared to the to wave elevation and its reference, without any control strategies applied to the buoy as depicted in Fig. 7. The buoy moves up and down on the surface of the

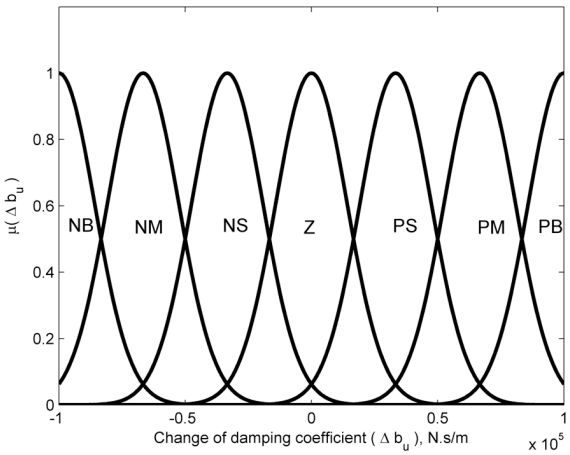

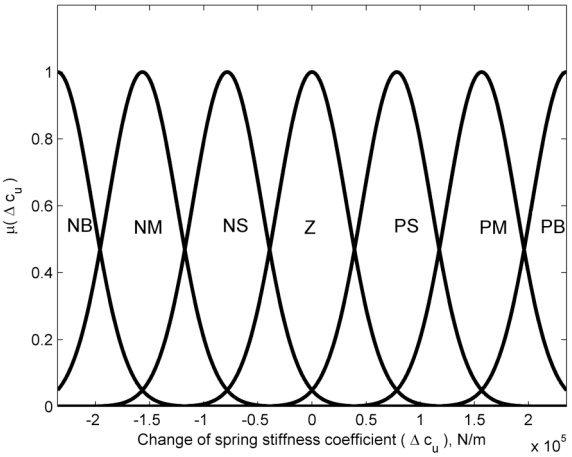

Fig. 6. Fuzzy sets for the output of the proposed FLC.

TABLE II
IF-THEN RULE FOR THE CALCULATION COEFFICIENTS OF b_u (UPPER) AND c_u (LOWER)

		e						
		PB	PM	PS	Z	NS	NM	NB
	NB	Z	PS	PS	PM	PM	PB	PB
	NM	NS	Z	PS	PS	PM	PM	PB
	NS	NS	NS	Z	PS	PS	PM	PM
$\dot{e}$	Z	NM	NS	NS	Z	PS	PS	PM
	PS	NM	NM	NS	NS	Z	PS	PS
	PM	NB	NM	NM	NS	NS	Z	PS
	PB	NB	NB	NM	NM	NS	NS	Z

		e						
		PB	PM	PS	Z	NS	NM	NB
	NB	Z	NS	NS	NM	NM	NB	NB
	NM	PS	Z	NS	NS	NM	NM	NB
	NS	PS	PS	Z	NS	NS	NM	NM
$\dot{e}$	Z	PM	PS	PS	Z	NS	NS	NM
	PS	PM	PM	PS	PS	Z	NS	NS
	PM	PB	PM	PM	PS	PS	Z	NS
	PB	PB	PB	PM	PM	PS	PS	Z

wave without any resonance happening between the velocity of the buoy and its reference. The low level of absorbed energy is resulted due to the inability of the buoy's velocity to follow its reference.

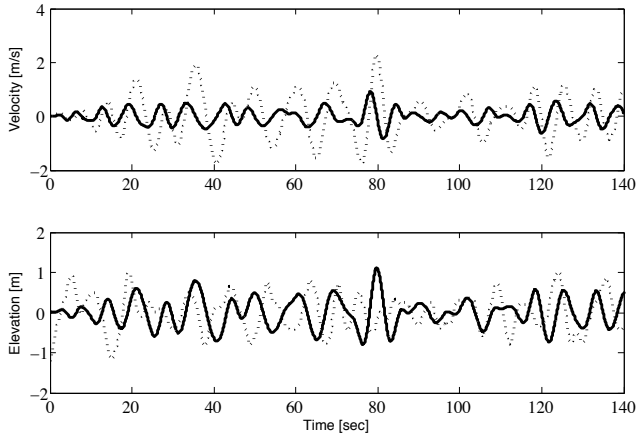

Fig. 7. The control simulation for the freely oscillating buoy. Upper graph is the buoy's velocity (solid) and its velocity (dotted). Lower graph is the buoy's elevation (solid) and the wave elevation(dotted).

The simulation result using the proposed FLC for the WEC in the case of nominal system is shown in Fig. 8. The information regarding the absolute value of maximum buoy's displacement and its control force can be found in Table III. From the two informations, we can see that the buoy relatively follows its reference velocity. The buoy still moves on the surface of the wave i.e., it is not totally jump or submerged from the surface of the water. The maximum level of the control force resulting from the FLC still in the reasonable level. As a comparison, the level of the excitation force f_e (one of the forces that acting on on the buoy) is in the order of 10^5 [N]. Therefore, the level of the control force from the FLC still reasonable.

The superior results can be obtained by applying the proposed SMC for the WEC as depicted in Fig. 9. The buoy almost perfectly tracks its reference velocity. This indicates a higher energy absorption by the PTO. From the information in Table III, the buoy's displacement is still within its allowable range. The maximum absolute value of

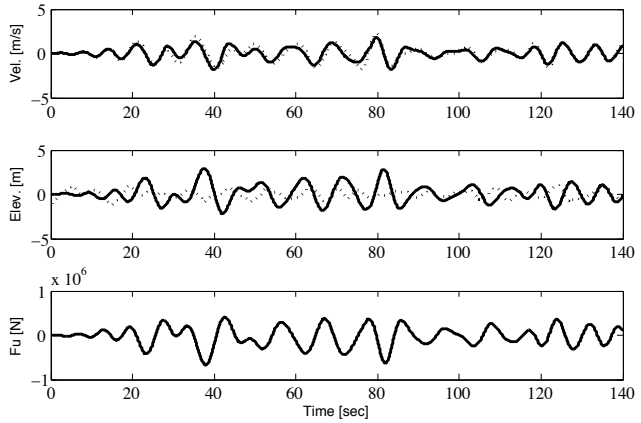

Fig. 8. The simulation results using the proposed FLC for the nominal case. Upper graph is the velocity of buoy (solid) and its reference (dotted). The middle graph is the buoy's elevation (solid) and the wave elevation (dotted). The lower graph is control force of the FLC.

TABLE III

ABSOLUTE VALUES OF THE MAXIMUM BUOY'S ELEVATION AND CONTROL FORCE

Scenario	Maximum Elevation	Maximum f_u
Nominal FLC	2.9 [m]	6.7 $\times 10^5$ [N]
Nominal SMC	3.3 [m]	9.0 $\times 10^5$ [N]
Perturb FLC	1.7 [m]	4.7 $\times 10^5$ [N]
Perturb SMC	3.5 [m]	1.4 $\times 10^6$ [N]

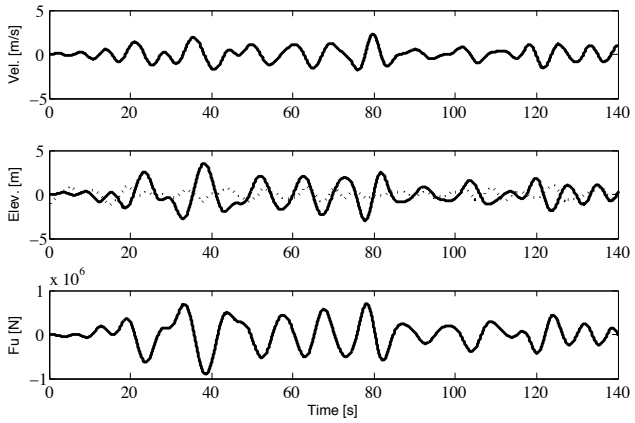

Fig. 9. The simulation results using the proposed SMC for the nominal case. Upper graph is the velocity of buoy (solid) and its reference (dotted). The middle graph is the buoy's elevation (solid) and the wave elevation (dotted). The lower graph is control force of the SMC.

the control force is also in the same level with f_e and the FLC.

Fig. 10 compares the energy absorption between the two proposed control strategies and no control strategy apply to the WEC for the nominal case. The calculation of the absorbed energy is based [22], and formulated as

$$W = (f_e - f_r)\dot{z}$$

where W is the energy in [W]. The proposed control strategies significantly improve the energy absorption from the

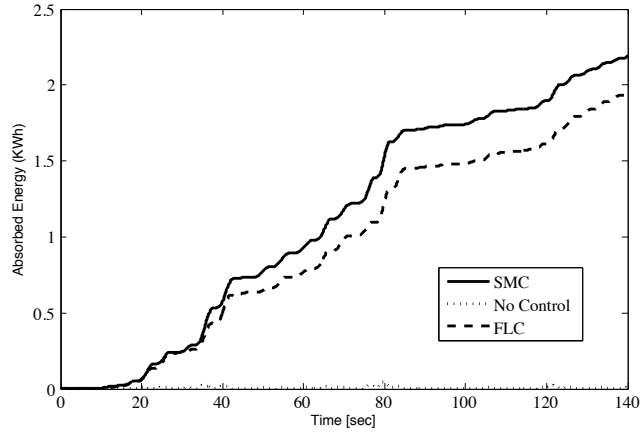

Fig. 10. The comparison the absorbed energy using the proposed methods and no control strategy for nominal case.

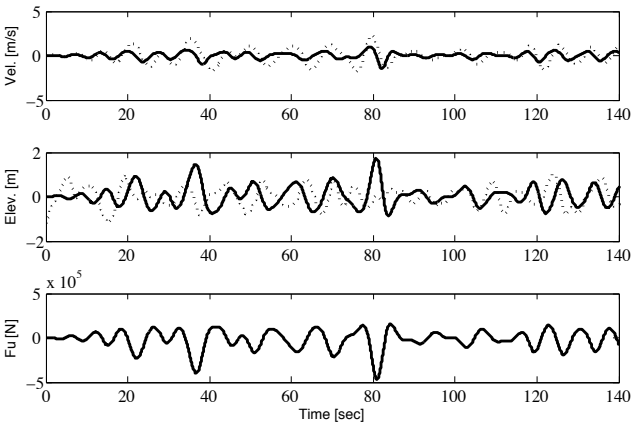

Fig. 11. The simulation results using the proposed FLC for the perturbation case. Upper graph is the velocity of buoy (solid) and its velocity reference (dotted). The middle graph is the buoy's elevation (solid) and the wave elevation (dotted). The lower graph is control force of the FLC.

WEC compared to the freely oscillating WEC. In particular, the SMC gives a larger energy absorption compared to the FLC because of the better tracking performance demonstrated by the SMC.

Next, we discuss the effect of perturbation on the WEC system. Here, we consider the perturbation happening due to an imprecise modeling of the WEC. We consider the perturbation of buoyancy coefficient c_b up to $+50\%$ from its nominal value. From practical point of view, this perturbation represents the change of the nominal c_b due to long operation in salty environment.

Fig. 11 shows the proposed FLC for the WEC under the perturbation scenario. Although the FLC still maintains the tracking capability within acceptable level, obviously there is a degradation on its tracking performance compared to the nominal case. The proposed FLC still maintains maximum absolute value of the control force and the buoy's elevation is within its allowable level as depicted in Table III.

Again, the superior performance is demonstrated by the

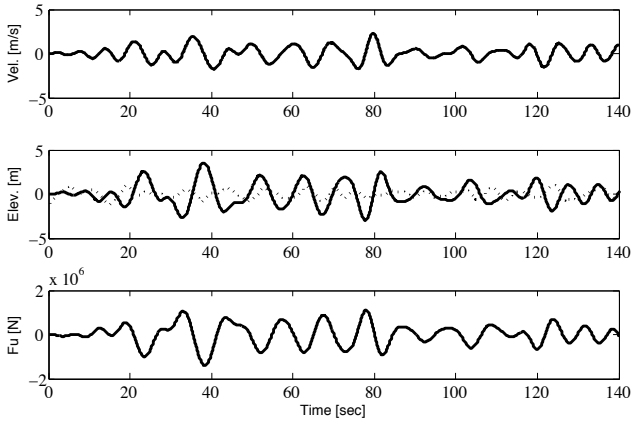

Fig. 12. The simulation results using the proposed SMC for the perturbation case. Upper graph is the velocity of buoy (solid) and its reference (dotted). The middle graph is the buoy's elevation (solid) and the wave elevation (dotted). The lower graph is control force of the SMC.

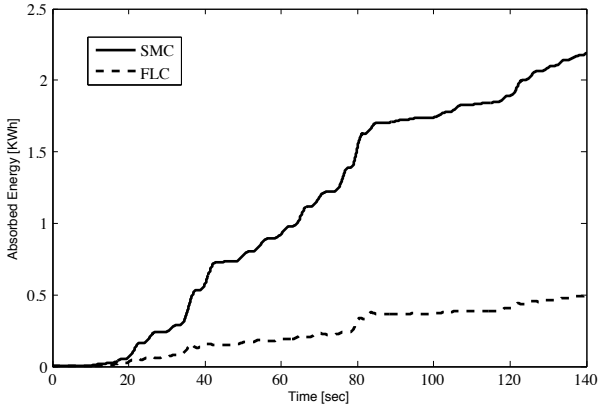

Fig. 13. The comparison the absorbed energy using the proposed FLC and SMC for perturbation case.

application of the proposed SMC for the perturbation case of the WEC as shown in Fig. 12. The tracking performance is successfully maintained similar to the nominal case. According to Table III, the maximum buoy's elevation always within its allowable range, while the maximum absolute value control force for the case with perturbation slightly higher compared to its nominal case, which defend on the selection of value of the parameter k. The maximum level of the control force can be reduced by decreasing the value of k. However, the smaller set of perturbation is obtained if we reduce the value of parameter k. In this case, we still can accept the maximum level of the control force. Therefore, we keep the value of parameter k so that it can handle larger perturbation set.

The energy absorption of the WEC with the perturbation is depicted in Fig. 13. The energy absorption of the WEC using the FLC decreases compared to the nominal case. Meanwhile, the proposed SMC maintains the level of energy absorption similar to the nominal case. This is because of its capability to track the reference despite the presence of uncertainty in the model of the WEC.

V. CONCLUSIONS

Two control strategies using the FLC and SMC are proposed in this paper. The proposed control strategies are tested using polychromatic wave to simulate the actual ocean environment. The maximum energy absorption is obtained by applying the proposed SMC to the WEC, compared to the FLC and free oscillating buoy in nominal and perturbed cases. This maximum energy absorption is achieved because the ability of proposed SMC to track its velocity reference in the nominal and perturbed cases. The maximum level of the control force and the buoy's elevation for the two proposed methods are always within the allowable ranges, limited by their physical considerations. Therefore, this research work provides the viable control solution for maximizing the energy absorption of the heaving WEC.

REFERENCES

[1] Cruz. J (editor), Ocean Wave Energy, Current status and future perspectives, Springer series in green energy and technology, Berlin, 2010.
[2] J. Falnes, A review of wave-energy extraction. Marine Structures, vol. 20, no. 4, pp. 185201, Oct. 2007.
[3] Sarpkaya. T and Isaacson M, Mechanics of Wave Forces on Offshore Structures. Van Nostrand Reinhold, New York, 1981.
[4] Falcao. O, Wave energy utilization: a review of the technologies, Journal of Renewable and Sustainable Energy Reviews, vol. 14, pp. 899-918, 2010.
[5] Budal K and Falnes J., Interacting point absorber with controlled motion, in the Power from Sea Waves, BM Count: Academic Press; 1980.
[6] K. Budal, J. Falnes, et al., The norwegian wave-power buoy project, The Second International Symposium on Wave Energy Utilization, Trondheim, June 1982.
[7] Babarit A, Duclos G, and Clement A. H, Comparison of latching control strategies for a heaving wave energy device in random sea, Journal of Applied Ocean Research, vol. 26, pp. 227-238, 2005.
[8] M. E. McCormick, Analysis of a wave energy conversion buoy, Journal of Hydronautics, vol. 8, no.3, pp.77 82, 1974.
[9] Schoen. M, J. Hals, and T. Moan, Wave Prediction and Robust Control of Heaving Wave Energy Devices for Irregular Waves, IEEE Trans. on Energy Conversion, Vol. 26, No. 2, 2011.
[10] M. A. Jama, A. Assi, Addy W., and H. Noura, Self-Tunable Fuzzy Logic Controller for the Optimization of Heaving Wave Energy Converters, The International Conference on Renewable Energy Research and Applications, 2012.
[11] M. A. Jama, A. Assi, Addy W., and H. Noura, Fuzzy Logic Based Controller for Heaving Wave Energy Converters, International Conference on Renewable Energies for Developing Countries, 2012.
[12] P. Gieske, Model predictive control of a wave energy converter: Archimedes Wave Swing. Masters thesis, Delft University of Technology, Delft, 2007.
[13] Brekken T, On model predictive control for a point absorber wave energy converter, IEEE Trondheim Power Tech, 2011.
[14] M. A. Jama, Addy W., A. Assi, and H. Noura, Controlling Heaving Wave Energy Converter using Function-Based Model Predictive Control Technique, Chinese Control and Decision Conference, 2013.
[15] Cummins. W. The impulse response functions and ship motions. Schiffstechnik, vol. 9, pp. 101109, 1661.
[16] Taghipoura. R, Pereza. T, and Moan. T. Hybrid frequency time domain models for dynamic response analysis of marine structures. Ocean Engineering, 35, pp.685705, 2008.
[17] G. D. Backer, Hydrodynamic Design Optimization of Wave Energy Converters Consisting of Heaving Point Absorbers Power, Dissertation submitted to obtain the academic degree of Doctor of Civil Engineering. 2010.
[18] WAMIT, "User Manual 2006", www.wamit.com, (accessed 20/01/2012).
[19] Addy W., M. A. Jama,A. Assi, and H. Noura, Sliding Mode Control for Heaving Wave Energy Converter, IEEE Multi-Conference on Systems and Control, 2013.
[20] MATLAB: The Language of Technical Computing, www.mathworks.com.
[21] J. Slotine and W. Li, Applied Nonlinear Control, Prentice Hall, 1991.
[22] J. Falnes, Ocean Waves and Oscillating Systems: Linear Interactions including Wave-energy Extraction, Cambridge Press, 2004.